ЖУРНАЛ СТРУКТУРНОЙ ХИМИИ

2017. Том 58, № 4 *Май – июнь* *С. 819 – 826*

UDC 543.422:548.737:547.573

EFFECT OF PROTONATION ON THE STRUCTURE OF 1,3,6,8-TETRAAZATRICYCLO[4.4.1.1^{3,8}]DODECANE (TATD) ADAMANZANE: CRYSTAL STRUCTURE AND DFT ANALYSIS OF 3,6,8-TRIAZA-1-AZONIATRICYCLO[4.4.1.1^{3,8}]DODECANE 4-NITROPHENOLATE 4-NITROPHENOL

A. Rivera[1], J.M. Uribe[1], J. Ríos-Motta[1], M. Bolte[2]

[1]*Universidad Nacional de Colombia, Sede Bogotá, Facultad de Ciencias, Departamento de Química, Bogotá, Colombia*
E-mail: ariverau@unal.edu.co (A. Rivera)
[2]*Institut für Anorganische Chemie, J. W. Goethe-Universität Frankfurt, Frankfurt/Main, Germany*

Received June, 25, 2015 *Revised — November, 30, 2015*

The reaction between 1,3,6,8-tetraazatricyclo[4.4.1.1^{3,8}]dodecane (TATD) and 4-nitrophenol (4-NP) under solvent-free conditions results in the formation of a proton transfer (PT) complex, $(TATD)^{+}(4\text{-}NP)^{-}\cdot 4\text{-}NP$, (**3**). This is the first crystal structure of a PT complex of TATD, whose structure is stabilized by N^{+}—H···O and O^{-}···H—O hydrogen bonds. The characterization was performed using FTIR and ^{1}H NMR spectroscopy, and X-ray crystallography. From X-ray diffraction data collected at 173(2) K, it is concluded that it crystallizes in the monoclinic system (*C*2/*c* space group) containing one 4-nitrophenolate anion and one neutral 4-nitrophenol molecule. The stoichiometry of the proton transfer species in DMSO-d_6 solution is in agreement with the structural data. A combined theoretical and experimental correlation of the structural parameters of free and protonated TATD are in good agreement. The discrepancies in the C—C bond distances between the experimental and calculated results can be attributed to hyper-conjugative interactions and electron delocalization.

DOI: 10.15372/JSC20170421

K e y w o r d s: 1,3,6,8-tetraazatricyclo[4.4.1.1^{3,8}]dodecane, adamanzane, crystal structure, proton transfer, hydrogen bond, aminal cage, DFT calculations.

INTRODUCTION

Tricyclic alkanic tetraamine 1,3,6,8-tetraazatricyclo[4.4.1.1^{3,8}]dodecane (TATD, **1**) has an adamanzane cage structure containing four nitrogen atoms in an approximate tetrahedral arrangement around each nitrogen atom [1], and the four lone pairs of the nitrogen bridgehead are oriented outside the cavity [2]. Adamanzane (**adaman**tane + tetraa**za** + ami**ne**) is the simplified nomenclature suggested by Springborg for naming the tetraaza cages [2]. Theoretical studies of the molecular structure and stability of **1** and hypothetical TATD-H^{+} (**1H**$^{+}$) have been described by Galasso [3], who concluded that the conformational preferences remain unchanged upon protonation. Unfortunately, until now there have been no experimental data to support this conclusion due to the reactivity of TATD (**1**) toward acids and phenols [4—7]. As we described previously [8], for the 1:1 adduct of **1** and hydroquinone elucidated by X-ray crystal structure determination, the bond angles around the four nitrogen atoms are closer to estimated values for the free amine than those of monoprotonated adamanzane,

which is consistent with the absence of proton transference. Thus, the structure and conformation of this protonated adamanzane in the solid state has been unexplored until now.

During our previous research on Mannich-type reactions between TATD and phenols in basic media, we observed that the reaction with 2-nitrophenol resulted in decomposition of the aminal cage and did not obtain the compounds produced by aminomethylation [5]. This result can be explained by a proton transfer from 2-nitrophenol to **1** and subsequent decomposition of the protonated cage, most likely due to (**1H**$^+$) unstability [4].

We recently reported the synthesis and X-ray crystal structure of a salt between the (2*R*,7*R*)-1,8,10,12-tetraazatetracyclo[8.3.1.1.^{8,12}0^{2,7}]pentadecane (**2**) cage and 4-nitrophenol obtained when a new, simple method was attempted to synthesize Mannich bases in our laboratory [9]. This structure revealed the role of stereoelectronic effects such as the anomeric effect and secondary orbital overlap on the stability of the cation and changes in the structure of the aminal cage. Moreover, we studied the behavior of **1** and 4-nitrophenol under the aforementioned conditions. We found that **1** readily reacted with 2 equivalents of 4-nitrophenol to give the 3,6,8-triaza-1-azoniatricyclo[4.4.1.1^{3,8}]dodecane 4-nitrophenolate 4-nitropenol (**3**) derivative adduct.

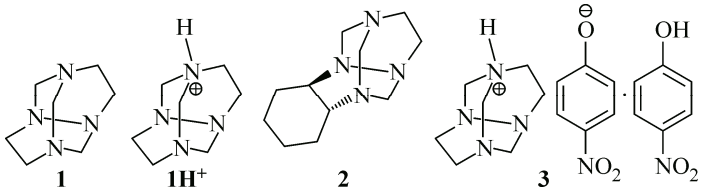

1 **1H$^+$** **2** **3**

EXPERIMENTAL

Physical measurements. TATD (**1**) was synthesized from formaldehyde and 1,2-diaminoethane as described in the literature [10], and 4-nitrophenol was purchased from Merck. The melting point was determined with an Electrothermal apparatus, and is uncorrected. IR spectrum was recorded in KBr pellets at 292 K on a Thermo Nicolet IS10 spectrophotometer. NMR experiments were performed in DMSO-d_6 at room temperature on a Bruker Avance AV-400 MHz spectrometer operated at 400 MHz for ^{1}H.

Preparation of the title compound. The synthesis of the title compound was performed under solvent-free conditions, as follows: a mixture of TATD (0.168 g, 1 mmol) and 4-nitrophenol (0.278 g, 2 mmol) was heated for 10 min at 323 K without any solvent. Once cooled to room temperature, the reaction mixture was extracted with chloroform and the chloroform extract was washed with benzene (3×5 ml) and water (3×5 ml) and dried over anhydrous Na_2SO_4. Removal of the solvent *in vacuo* gave the title compound. Yield 75 %, m.p. = 362—363 K. ^{1}H NMR (DMSO-d_6, ppm): 3.10 (s, 8H), 3.78 (s, 8H), 6.72 (d, 4H, J = 8 Hz), 7.30 (d, 4H, J = 8 Hz). Crystals suitable for X-ray diffraction were obtained from MeOH upon slow evaporation of the solvent at room temperature.

X-ray crystallography. The X-ray diffraction data were collected on a STOE IPDS II two-circle diffractometer with MoK_α radiation (λ = 0.71073 Å) at 173(2) K in the ω scan mode. The structure was solved by direct methods using SHELX-97 [11]. For the structural refinement [11], the non-hydrogen atoms were treated anisotropically, and H atoms were treated by a mixture of independent and constrained refinement. C-bound H atoms were fixed geometrically (C—H = 0.95 to 0.99 Å) and refined using a riding model approximation, however, positions of the 4-nitrophenol hydrogen atom (O1—H1) and the nitrogen—hydrogen atom (N21—H21) were localized from difference Fourier map, their positions were freely refined without constraint on the distance to parent atoms. Crystallographic data (excluding structure factors) have been deposited at the Cambridge Crystallographic Data Centre. Copies of the data can be obtained free of charge on application to the CCDC, 12 Union Road, Cambridge CB2 IEZ, UK. Fax: +44-(0)1223-336033 or the structure can be downloaded from https://summary.ccdc.cam.ac.uk/structure-summary-form. The CCDC deposition number is 1054338. Crystal data and details concerning data collection and structure refinement are given in Table 1, and select bond distances are listed in Table 2.

Table 1

Crystal data and structure refinement for **3**

Empirical formula	$C_{20}H_{26}N_6O_6$
Temperature, K	173(2)
Formula weight	446.47
Wavelength, Å	0.71073
Crystal system	Monoclinic
Space group	*C*2/*c*
Unit cell dimensions: *a*, *b*, *c*, Å; β, deg.	21.231(3), 6.205(1), 32.002(4); 91.82(1)
Volume, Å^3	4213.4(11)
Z	8
Calculated density, g/cm^3	1.408
Absorption coefficient, mm^{-1}	0.106
F(000)	1888
Crystal size, mm	0.19×0.13×0.02
θ range for data collection, deg.	2.27—25.48
Limiting indexes	$-21 \le h \le 25$, $-6 \le k \le 7$, $-38 \le l \le 38$
Reflections collected / unique	11173 / 3890 [*R*(int) = 0.1132]
Completeness to θ = 25.00, %	99.8
Final shift/error, max and avg	0.000, 0.000
Refinement method	Full-matrix least-squares on F^2
Data / restraints / parameters	1570 / 0 / 297
Goodness of fit on F^2	0.786
Final *R* indices [$I > 2\sigma(I)$], %	*R*1 = 4.9, *wR*2 = 9.2
R indices (all data), %	*R*1 = 15.0, *wR*2 = 11.6
Largest peak and hole, e/Å^3	0.165 and –0.173

Table 2

Select bond lengths (Å) *for* **3**

O(1)—C(1)	1.347(4)	N(21)—H(21)	1.13(5)	N(23)—C(26)	1.450(5)
O(11)—C(11)	1.320(4)	N(22)—C(21)	1.399(4)	N(24)—C(22)	1.414(5)
O(11)—H(1)	1.47(5)	N(22)—C(27)	1.461(4)	N(24)—C(28)	1.461(5)
N(21)—C(25)	1.510(4)	N(22)—C(23)	1.469(4)	N(24)—C(24)	1.468(4)
N(21)—C(22)	1.542(4)	N(23)—C(23)	1.437(5)	C(25)—C(26)	1.499(5)
N(21)—C(21)	1.544(5)	N(23)—C(24)	1.448(4)	C(27)—C(28)	1.509(5)

Theoretical calculations. Calculations were performed using the Gaussian 03 package [12]. The initial geometries of free (**1**) and protonated (**1H**$^+$) structures generated from single crystal XRD data were optimized at the DFT level of theory, with the B3LYP exchange correlation functional and the 6-31G+(*d*,*p*) basis set [13—15].

RESULTS AND DISCUSSION

Initially, IR spectra (Fig. 1) of the reaction product, prepared as KBr pellets of the solid, were acquired for qualitative identification. The main bands in these spectra were stretching vibrations of OH groups in the 3750 to 3000 cm^{-1} range, which overlapped with the C—H stretching of aromatic rings (ν = 2950 cm^{-1}) and the stretching vibration of the C—H bond in —CH_2CH_2— (ν = 2924 cm^{-1}) and —NCH_2N— (ν = 2875 cm^{-1}) groups. Bending vibrations of methylene groups were also visible at

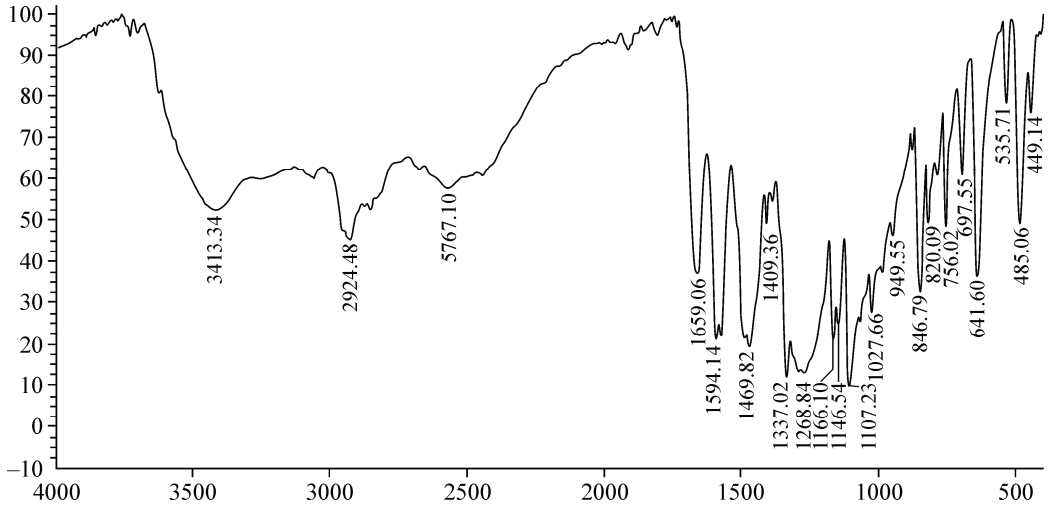

Fig. 1. FTIR spectrum of **3** in KBr

$\nu = 1337\ cm^{-1}$, and aromatic ring C=C stretching was found at $1659\ cm^{-1}$. The strong absorptions at $1470\ cm^{-1}$ and $1269\ cm^{-1}$ were attributed to the asymmetric and symmetric stretching vibrations of NO_2 groups. The aromatic C—O vibration occurred at $1166\ cm^{-1}$. Taken together, these data strongly suggest the presence of both a caged aminal polyamine and a 4-nitrophenol unit in the reaction product.

The O—H stretching vibration in 4-nitrophenol is typically observed in the $3325\ cm^{-1}$ region [16]. However, in the present case, the infrared spectra of the product display a medium-strong broad absorption at $3413\ cm^{-1}$, which corresponds to the hydrogen bonded O—H stretching vibration. This ″anomalous blue shift″ of the O—H stretching wavenumber is due to strong inter- or intramolecular ″improper blue-shifting hydrogen bonding″ [17]. Furthermore, the IR spectrum has another broad signal centered at $2567\ cm^{-1}$ that is the characteristic vibration for the N^+—H bond in a protonated tertiary amine group. However, comparison of the frequency calculated in the gas phase at the B3LYP level by Galasso ($3426\ cm^{-1}$) [3] with our experimental data reveals the overestimation of the calculated vibrational mode. This overestimation was due not only to neglect of anharmonicity in the real system but also to the possible existence of a strong hydrogen bond between the cation and 4-nitrophenolate. Thus, and because O—H group vibrations are likely to show shifts in the spectra of the hydrogen bonded species, the observation of two distinct broad signals has been rationalized as the existence of various hydrogen-bonded structures. Specifically, extended hydrogen-bound 4-nitrophenol structures are assigned to the broad absorption centered at $3413\ cm^{-1}$, and an asymmetric hydrogen bond having two different hydrogen-bond donors and acceptors is assigned to the absorption band at $2567\ cm^{-1}$. However, the nature of the hydrogen bond in this aggregate is not clear, because we have no way to distinguish between a hydrogen bond and a structure resulting from proton transfer.

However, in contrast to the presence of N^+—H frequencies in FTIR and although the shift and integration values of the ^{1}H-NMR data in DMSO-d_6 indicated that a 1:2 adduct was present in the reaction product, two nonequivalent hydrogens were present in the aliphatic region that appeared as two singlets with chemical shifts surprisingly similar to those of the free amine. Moreover, we did not detect any decomposition of the material submitted to NMR. Thus, in DMSO, equilibrium exists only between the free amine and 4-nitrophenol. However, FT-IR and NMR spectra cannot provide a firm conclusion about structural changes in the aminal cage.

In the second stage of this work, which was stimulated by these spectral results, we searched for alternative methods to obtain crystals of sufficient quality to collect experimental data, in order to compare with previously published theoretical data [3].

As shown in Fig. 2, adduct **3** crystallizes in the monoclinic system. The structure of **3** was solved in the *C*2/*c* space group. The asymmetric unit of **3** comprises one 3,6,8-triaaza-1-zoniatricyc-

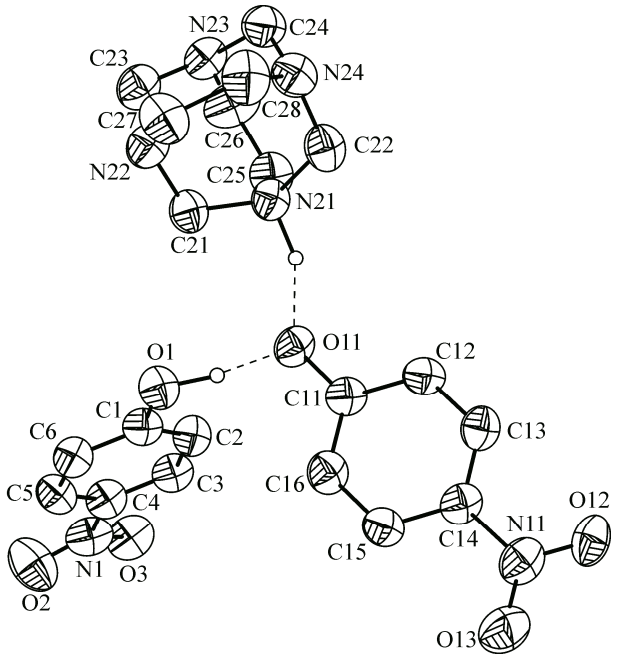

Fig. 2. The molecular structure of the title adduct. Displacement ellipsoids are drawn at the 50 % probability level.
H atoms bonded to C atoms are omitted for clarity. Hydrogen bonds are drawn as dashed lines

lo[4.4.1.1^{3,8}]dodecane mono cation, one 4-nitrophenolate anion, and one neutral 4-nitrophenol molecule (Fig. 2). The acidic proton of one 4-nitrophenol is completely transferred to one TATD nitrogen atom, and there is a hydrogen-bonding interaction between the cationic and anionic species (N···O, 2.667(4) Å). Furthermore, this strong interaction is assisted by another O—H···O hydrogen bond originating from the OH group of the neutral 4-nitrophenol towards phenolate oxygen atom O11 (O···O, 2.526(4) Å), forming a supramolecular structure (Table 3). The crystal structure is stabilized by intermolecular hydrogen bonding and the geometric details of these bonds are listed in Table 3. The most notable feature in the cation is the elongation of the N21—C bond lengths (1.510(4) Å, 1.542(4) Å, and 1.544(5) Å) as well as the shortening of the N—CN21 bond lengths (1.399(4) Å and 1.414(15) Å) compared to other N—C bond lengths (1.437(5) Å to 1.469(4) Å), which is consistent with protonation at the N21 atom. In the anion, the C11—O11 and C1—O1 bond lengths of 1.320 (4) Å and 1.347 (4) Å are shorter by 0.039 Å and 0.012 Å respectively, than those in the X-ray structure of the stable α-modification of 4-nitrophenol (1.359(1) Å) [18], which is also consistent with proton transfer and hydrogen bonding, respectively (Table 3).

Inversion dimers of the co-crystalline adduct linked by pairs of C—H···O hydrogen bonds generate a $R_2^2(26)$ motif with C25—H25B···O2^{i} = 3.239(5) Å (symmetry code: ^{i} –*x*+3/2, –*y*+1/2, –*z*+1) (Table 3, Fig. 3). These are further connected by C—H···O interactions (C22—H22A···O12^{ii} = = 3.343(5) Å), and these combine with the aromatic C6—H6···O11 contacts to link alternating pairs of dimers into undulated layers parallel to the *bc* plane (Fig. 4). Additionally, a C—H···π interaction is observed between the centroid of the nitrophenolate ring (C11—C16) and a hydrogen of the neighbouring nitrophenolate ring (C13—H13···π).

Table 3

Hydrogen bond geometry (Å, deg.), *for* **3**. Cg *is the centroid of the* C11—C16 *phenyl ring*

Entry	*d*			Angle
	D—H	H···A	D···A	D—H···A
O1—H21···O11	1.07(5)	1.47(5)	2.526(4)	171(4)
N21—H21···O11	1.13(5)	1.59(5)	2.667(4)	156(4)
C6—H6···O11^{i}	0.99	2.56	3.461(6)	151
C22—H22A···O12^{ii}	0.99	2.56	3.461(6)	151
C25—H25B···O2^{iii}	0.99	2.56	3.461(6)	151
C13—H13···*Cg*^{iv}	0.95	2.88	3.547 (4)	128

Symmetry codes: ^{i} *x*, *y*–1, *z*; ^{ii} *x*–3/2, *y*–1/2, 3/2–*z*; ^{iii} *x*–3/2, 1/2–*y*, 1–*z*, ^{iv} –*x*+3/2, *y*+1/2, –*z*+3/2.

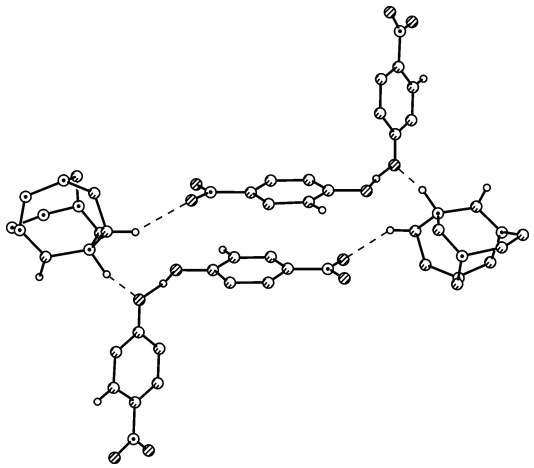

Fig. 3. Supramolecular structure of an inversion dimer of the title compound

Motivated by this result, we commenced a broader study by combined theoretical and experimental investigation of the structural consequence of the protonation of TATD (**1**), a small aminal cage tetraamine. We compared the experimental crystal structure to the optimized structure of $\mathbf{1H}^+$ and **1**.

Previously, in a related computational investigation in the same chemical system, Galasso studied the structural and spectroscopic properties of free and protonated adamanzanes [3]. He found that the use of the B3LYP/6-31+G(*d*,*p*) functional provides a good compromise between the size of the calculations and the accuracy of the theoretical predictions. Thus, based on the X-ray coordinates for TATD [19] and monoprotonated TATD, a full geometry optimization of the systems in a vacuum and the molecular structure parameters of TATD-H+ and TATD were calculated by density functional theory (B3LYP) with the 6-31+G(*d*,*p*) basis set [13—15]. The calculated molecular structure parameters were analyzed and compared with the obtained experimental data. Both the selected experimental bond lengths, bond angles and dihedral angles and those calculated by B3LYP/6-31+G(*d*,*p*) are listed in Table 4.

From the data (Table 4), through comparison of the results obtained by DFT calculations and the previous experimental data for the free amine, several observations can be made. The experimental C—C bond length in the ethylene bridge is 1.477(8) Å, whereas this value was calculated as 1.569 Å. The NCH_2CH_2—N and NCH_2—N bond lengths are 1.460 Å and 1.466 Å, respectively, which agree with the experimental values of 1.459 Å and 1.456 Å and are slightly smaller than the normal C—N single bond length of approximately 1.469 Å [20].

For the monoprotonated species, the calculated results show that the optimized geometry closely reproduces the crystal structural geometry; for example, the bond lengths agree with those obtained from the crystallographic data (the mean absolute deviation of bond distances is 0.032 Å). However, the most notable difference between the X-ray crystallographic data and the B3LYP/6-31+G(*d*,*p*)-optimized model is the shortening of the C—C and NCH_2—N^+ bonds. When comparing the experi-

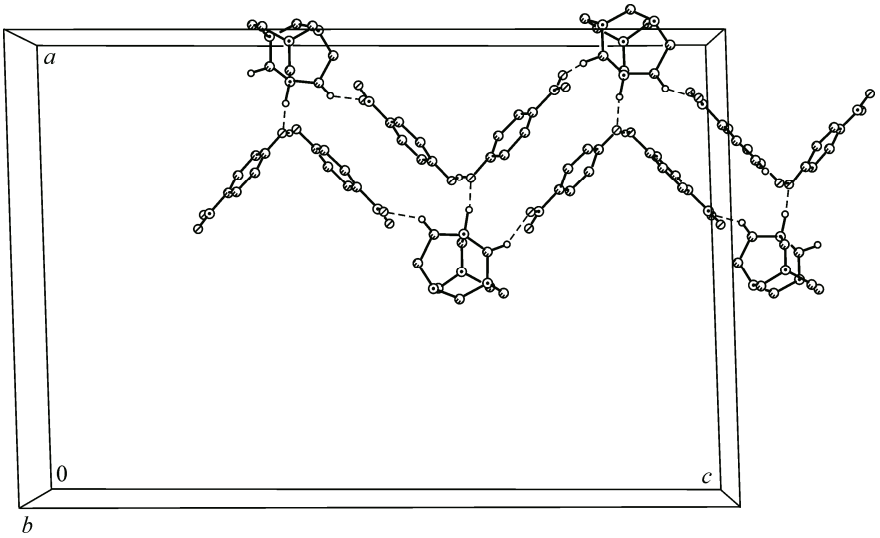

Fig. 4. The crystal packing of the title compound, showing layers parallel to the *ab* plane. Hydrogen bonds are drawn as dashed lines. H atoms not involved in hydrogen bonds are omitted

Table 4

Structural parameters of free (**1**) *and protonated* TATD (**1H**$^+$)
(*distances in* Å *and bond angles*, *sum of bond angles and torsion angles in* deg.)

Parameter		**1**		**1H**$^+$	
		exp[a]	theo[b,c]	exp[c]	theor[b,c]
*d*C—C	NCH_2—CH_2N	1.477(8)	1.569	1.499(5)	1.567
	NCH_2—CH_2N^+	—	—	1.509(5)	1.564
*d*C—N	NCH_2CH_2—N	1.459(5)	1.460	1.450(4) and 1.461(5)	1.455 and 1.464
	NCH_2CH_2—N^+	—	—	1.510(4)	1.508
	NCH_2—N	1.456(2)	1.466	1.437(5) to 1.469(4)	1.457 and 1.476
	NCH_2—N^+	—	—	1.542(4) and 1.544(5)	1.603
	N^+CH_2—N	—	—	1.399(4) and 1.414(15)	1.399
*d*N—H	N^+—H	—	—	1.13(5)	1.026[b,c]
α	N—C—N	119.4(3)	118.3	117.9(3) and 117.2(3)	115.5 and 115.6
	N—C—N^+	—	—	118.5(3) and 116.7(3)	115.8 and 115.9
	N—C—C	117.68(18)	115.4	115.2(3), 117.1(3) and 118.9(3)	114.0, 114.1 and 117.5
	N^+—C—C	—	—	114.3(3)	113.3
∑α	C—N—C	342.32	345.0[b,c]	345.4, 346.2 and 346.6	347.8, 350.2 and 350.1
	C—N^+—C	—	—	340.0	339.8[b,c]
	H—N^+—C	—	—	315.8	316.1[b,c]
Torsion angle	N—C—C—N	0	0	–1.2(6)	–4.6
	N—C—C—N^+	—	—	8.3(6)	5.3

[a] Ref [19].
[b] Ref [3].
[c] This work.

mental with the theoretical C—C and NCH_2—N^+ bond lengths; the calculated bond lengths are always higher than the experimental values. In contrast, the optimized structures yield identical bond lengths for the N^+CH_2—N bonds and the values calculated by the 6-31+G(*d*,*p*) basis set are the most similar to experimental values.

The optimized structures of both species exhibit typical Csp^3—Csp^3 single bond lengths ranging from 1.564 Å to 1.569 Å, with similar values for both free and monoprotonated TATD, which have a near normal C—C bond distance (1.524 Å) [20], and agree with the C—C bond length observed in ethylenediamine (1.51 Å) [21]. However, the experimental data ranges from 1.477 Å to 1.509 Å, and the bond lengths of the C—C bond in monoprotonated TATD are 1.499(5) Å and 1.509(5) Å, which are much longer than the C—C bond in the free amine (1.477(8) Å). The DFT method definitely overestimated the length of the ethylene bridge C—C bond distances in the adamanzane cage structure and also suggests remarkable conjugation effects.

CONCLUSIONS

The present paper reports on the synthesis and crystal structure of 1:2 co-crystalline adduct of TATD and two 4-nitrophenol molecules, containing one 4-nitrophenolate anion and one neutral 4-nitrophenol molecule $(TATD)^+(4\text{-}NP)^-\cdot 4\text{-}NP$. The adduct crystallizes via proton transference and strong intermolecular hydrogen bonds. This is the first example of a stable salt of this azaadamantane structure. The DFT analysis consolidates experimental and theoretical data, and as a result of the calculations performed, it is found that a comparison of C—N bond lengths around the protonated N atom in the aminal cage shows lengthening of C—N^+ and shortening of N^+C—N and the anomeric

effect cause changes in bond lengths. The results reported herein should contribute significantly toward the use of crystalline adducts of macrocyclic aminals for studying the generalized anomeric effect in aminals.

We acknowledge the Dirección de Investigaciones, Sede Bogotá (DIB) de la Universidad Nacional de Colombia, for financial support of this work. JMU thanks COLCIENCIAS for a fellowship.

REFERENCES

1. *Murray-Rust P.* // J. Chem. Soc. Perkin Trans. II. – 1974. – P. 1136 – 1141.
2. *Springborg J.* // Dalton Trans. – 2003. – P. 1653 – 1665.
3. *Galasso V.* // Chem. Phys. – 2001. – **270**. – P. 79 – 91.
4. *Simkins R.J., Wright G.F.* // J. Am. Chem. Soc. – 1955. – **77**. – P. 3157 – 3159.
5. *Rivera A., Ríos-Motta J., Navarro M.A.* // Heterocycles. – 2006. – **68**. – P. 531 – 537.
6. *Rivera A., Ríos-Motta J., Quevedo R., Joseph-Nathan P.* // Rev. Colomb. Quim. – 2005. – **34**. – P. 105 – 115.
7. *Rivera A., Gallo G.I., Gayón M.E., Joseph-Nathan P.* // Synth. Commun. – 1993. – **23**. – P. 2921 – 2929.
8. *Rivera A., Ríos-Motta J., Hernández-Barragán A., Joseph-Nathan P.* // J. Mol. Struct. – 2007. – **831**. – P. 180 – 186.
9. *Rivera A., Uribe J.M., Ríos-Motta J., Osorio H.J., Bolte M.* // Acta Crystallog. – 2015. – **C71**. – P. 284 – 288.
10. *Bischoff C.A.* // Ber. Dtsch. Chem. Ges. – 1898. – **31**. – P. 3248 – 3258.
11. *Sheldrick G.M.* SHELX-97. Program for the refinement of the crystal structures. – University of Göttingen, Germany, 1997.
12. *Frisch M.J., Trucks G.W., Schlegel H.B. et al.* Gaussian 03 (Revision E0.1), Gaussian Inc., Pittsburgh, PA, 2007.
13. *Becke A.D.* // Phys. Rev. A. – 1988. – **38**. – P. 3098 – 3100.
14. *Becke A.D.* // J. Chem. Phys. – 1993. – **98**. – P. 5648 – 5652.
15. *Lee C., Yang W., Parr R.G.* // Phys. Rev. B. – 1988. – **37**. – P. 785 – 789.
16. *Gandhimathi R., Dhanasekaran R.* // IOP Conf. Ser.: Mater. Sci. Eng. – 2013. – **43**. – P. 012004. doi:10.1088/1757-899X/43/1/012004.
17. *Joseph J., Jemmis E.D.* // J. Am. Chem. Soc. – 2007. – **129**. – P. 4620 – 4632.
18. *Kulkarni G.U., Kumaradhas P., Rao C.N.R.* // Chem. Mater. – 1998. – **10**. – P. 3498 – 3505.
19. *Rivera A., Ríos-Motta J., Bolte M.* // Acta Crystallog. – 2014. – **E70**. – P. o266.
20. *Allen F.H., Kennard O., Watson D.G., Brammer L., Orpen A.G., Taylor R.* // J. Chem. Soc. Perkin Trans. 2. – 1987. – P. S1 – S19.
21. *Jamet-Delcroix P.S.* // Acta Crystallog. – 1973. – **B29**. – P. 977 – 980.
22. *Hoffmann R.* // Acc. Chem. Res. – 1971. – **4**. – P. 1.
23. *Rathna A., Chandrasekhar J.* // J. Chem. Soc., Perkin Trans. – 1991. – **2**. – P. 1661.
24. *Palenik G.J., Koziol A.E., Katritzky A.R., Fan W.Q.* // J. Chem. Soc., Chem. Commun. – 1990. – P. 715.
25. *Ji L., Fang Q., Fan J.* // Acta Crystallog. E. – 2009. – **65**. – P. o136.
26. *Foster J.P., Weinhold F.* // J. Am. Chem. Soc. – 1980. – **102**. – P. 7211.